

# The Influence of Metallization Thickness on the Characteristics of Cascaded Junction Discontinuities of Shielded Coplanar Type Transmission Line

Tian-Wei Huang and Tatsuo Itoh, *Fellow, IEEE*

**Abstract**—A full-wave analysis based on the mode-matching technique is applied to analyze cascaded junction discontinuities of coplanar type transmission lines, coplanar waveguide (CPW) and finline. Results for a CPW-finline transition, a shielded CPW gap and a symmetric notch incorporating the finite metallization thickness effect are presented. The influence of metallization thickness on the coupling effect between cascaded junction discontinuities is also presented and discussed for the first time.

## I. INTRODUCTION

WHEN THE dimensions of the monolithic microwave integrated circuit (MMIC) become smaller, the coupling effect between cascaded junction discontinuities becomes significant. For such small waveguide dimensions, the effect of finite metallization thickness cannot be neglected. Although the metallization thickness effect of uniform transmission lines or single discontinuity circuits has been analyzed by many other authors [1]–[6], no one has included the finite-thickness effect in the analysis of cascaded discontinuities circuits. This paper uses several practical structures, such as CPW-finline transition [7], CPW gap, and symmetric notch, to demonstrate the influence of metallization thickness on cascaded discontinuities in circuits.

The metallization thickness effect is related to the percentage of field energy stored in the dielectric substrate [2]. A thicker metallization concentrates more field in slots [1] and reduces the percentage of the field energy stored in the dielectric, which results in a decreased effective dielectric constant. The effect of metallization thickness can be easily demonstrated by structures which have a moderate percentage of field energy stored in the dielectric, like a shielded structure operating in the waveguide band [1] or an open structure operating at medium frequencies [4], [5]. On the contrary, for an open structure operating at extremely high frequencies [5], the dielectric contains an extremely high percentage of field energy. With an extreme percentage of energy stored in the dielectric, the effect of thick metallization on the field is reduced; therefore, the influence of the metallization thickness on the propagation properties is quite small. For example, a shielded waveguide structure operating near the waveguide

cutoff frequency, an enclosed slot with metallization thickness behaves as a ridged waveguide [1], which has a totally different influence on the propagation properties from those discussed above. In this case, by increasing the metallization thickness, the effective dielectric constant is decreased near the cutoff frequency, but increased at higher frequencies. This behavior indicates the existence of an intersection near the cutoff frequency, and an increasing thickness effect at higher frequency.

According to the above discussion, a WR-28 waveguide shielded structure operating in the waveguide band (*Ka*-band) is selected to demonstrate the effect of finite metallization thickness. Kuo [3] has used the same structure to show the finite metallization thickness effect on single discontinuity circuits. A parallel-plate waveguide model was proposed by him to explain the increased power transmitted through the slot for a thicker metallization. This paper extends his method to analyze cascaded junction discontinuities incorporating the finite metallization thickness effect. The influence of metallization thickness on the coupling effect between cascaded junction discontinuities is also presented for the first time.

## II. MODE- MATCHING TECHNIQUE

Before applying the mode-matching technique, the extended spectral domain approach [1] is used to calculate the eigenmodes of each transmission line incorporating the finite metallization thickness effect. The geometry of the problem is shown in Fig. 1. A CPW-finline transition consisting of cascaded discontinuities is shielded by a WR-28 rectangular waveguide. Imposing the continuity of tangential field at both discontinuities,  $z = 0$  and  $z = L_0$ , a set of simultaneous equations (1a)–(d) can be expressed as

$$\vec{e}_1^a + \sum_{n=1}^{\infty} a_n \vec{e}_n^a = \sum_{n=1}^{\infty} c_n \vec{e}_n^g + \sum_{n=1}^{\infty} d_n \vec{e}_n^g \quad (1a)$$

$$\vec{h}_1^a - \sum_{n=1}^{\infty} a_n \vec{h}_n^a = \sum_{n=1}^{\infty} c_n \vec{h}_n^g - \sum_{n=1}^{\infty} d_n \vec{h}_n^g \quad (1b)$$

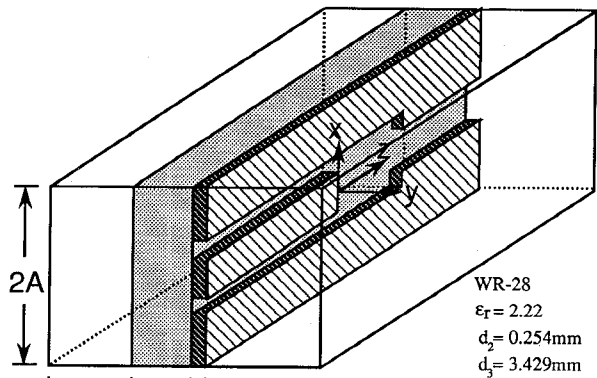
$$\begin{aligned} \sum_{n=1}^{\infty} b_n \vec{e}_n^b e^{-\gamma_n^b L_0} &= \sum_{n=1}^{\infty} c_n \vec{e}_n^g e^{-\gamma_n^g L_0} \\ &+ \sum_{n=1}^{\infty} d_n \vec{e}_n^g e^{+\gamma_n^g L_0} \end{aligned} \quad (1c)$$

Manuscript received March 30, 1992; revised August 3, 1992.

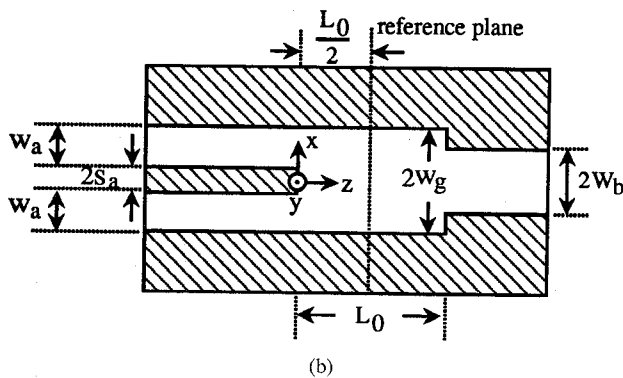
This work was supported by the TRW MICRO program and the Office of Naval Research N00014-91-J-1651.

The authors are the Department of Electrical Engineering, University of California at Los Angeles, Los Angeles, CA 90024.

IEEE Log Number 9206298.



(a)



(b)

Fig. 1. (a) Shielded CPW-finline transition including cascaded discontinuities with the finite metallization thickness, (b) longitudinal section.

$$\sum_{n=1}^{\infty} b_n \vec{h}_n^b e^{-\gamma_n^b L_0} = \sum_{n=1}^{\infty} c_n \vec{h}_n^g e^{-\gamma_n^g L_0} - \sum_{n=1}^{\infty} d_n \vec{h}_n^g e^{+\gamma_n^g L_0} \quad (1d)$$

where

$a, g, b$  are the left, center and right section of cascaded discontinuities

$a_n, b_n, c_n, d_n$  are the expansion coefficient of each eigenmode

$\vec{e}_n, \vec{h}_n$  are the normalized transverse vector electrical and magnetic fields

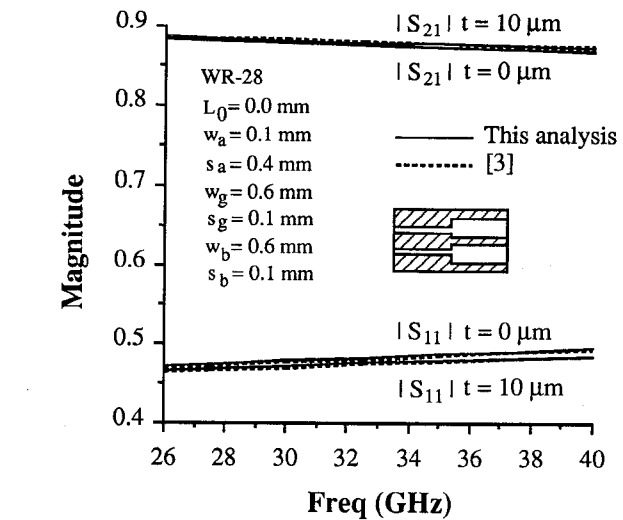


Fig. 2. Comparison of results for a CPW step discontinuity with metallization thickness.

The  $x, y$  dependence of the above simultaneous equations can be eliminated by an inner product (3). This process results in a system of linear equations (2a)–(d) with some unknown modal coefficients,  $a_n, b_n, c_n, d_n$ . For the numerical computation, only a finite number of modes,  $N_a, N_b$  and  $N_g$  are used to solve this linear system, shown in (2a)–(2d) at the bottom of the page, where

$$I_{mn}^{fp} = \int_s \vec{e}_m^f \times \vec{h}_n^{p*} \cdot \hat{z} dS, \quad f, p \in \{a, g, b\} \quad (3)$$

The selection of  $f, p$  in the inner product (3) depends on the structure of cascaded discontinuities. For example, (2a)–(d) are designed for a structure with an enlarged boundary at its first discontinuity and a reduced boundary at the second. For a given junction discontinuity, to select the electric field from the small aperture section and magnetic field from the large aperture section in the inner product (3) will produce a convergent result with a minimum number of modes [8].

### III. NUMERICAL RESULTS

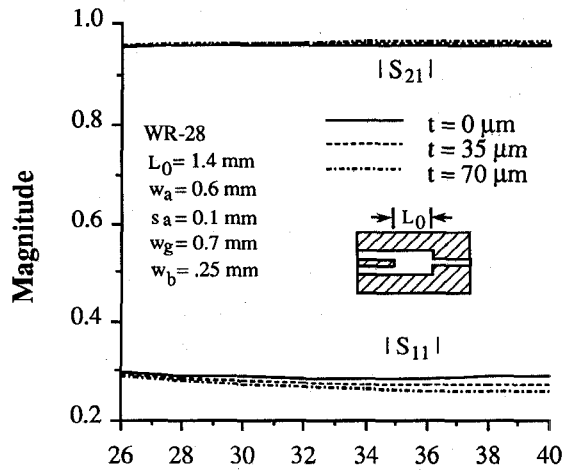
A computer code for the coplanar type transmission line cascaded junction discontinuities was developed and checked with

$$\sum_{n=1}^{N^a} a_n I_{nm}^{ag} + 0 - \sum_{n=1}^{N^g} c_n I_{nm}^{gg} - \sum_{n=1}^{N^g} d_n I_{nm}^{gg} = -I_{1m}^{ag} \quad m = 1, \dots, N^g \quad (2a)$$

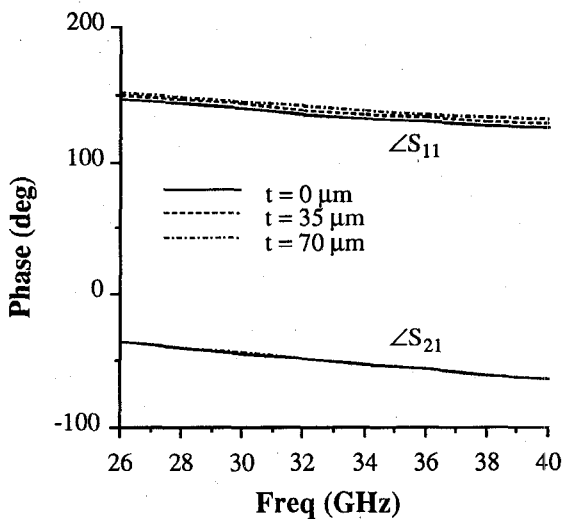
$$\sum_{n=1}^{N^a} a_n I_{mn}^{aa} + 0 + \sum_{n=1}^{N^g} c_n I_{mn}^{ag} - \sum_{n=1}^{N^g} d_n I_{mn}^{ag} = +I_{m1}^{aa} \quad m = 1, \dots, N^a \quad (2b)$$

$$0 + \sum_{n=1}^{N^b} b_n I_{nm}^{bg} e^{-\gamma_n^b L_0} - \sum_{n=1}^{N^g} c_n I_{nm}^{gg} e^{-\gamma_n^g L_0} - \sum_{n=1}^{N^g} d_n I_{nm}^{gg} e^{+\gamma_n^g L_0} = 0 \quad m = 1, \dots, N^g \quad (2c)$$

$$0 + \sum_{n=1}^{N^b} b_n I_{mn}^{bb} e^{-\gamma_n^b L_0} - \sum_{n=1}^{N^g} c_n I_{mn}^{bg} e^{-\gamma_n^g L_0} + \sum_{n=1}^{N^g} d_n I_{mn}^{bg} e^{+\gamma_n^g L_0} = 0 \quad m = 1, \dots, N^b \quad (2d)$$



(a)

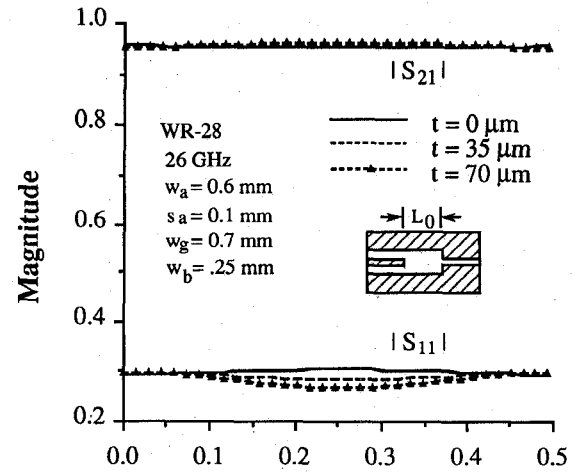


(b)

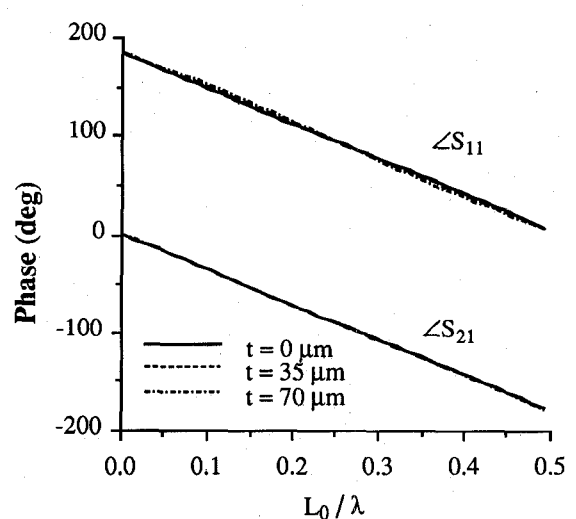
Fig. 3. Scattering parameters of a CPW-finline transition for a coupled-slot mode incident at  $L_0 = 1.4$  mm, (a) magnitude, (b) phase.

published results [3] in Fig. 2. After several extensive convergence tests, six eigenmodes in each transmission line section are selected to be used in the mode-matching techniques, i.e.,  $N_a = N_g = N_b = 6$ . There is only 0.01% of relative error between 6 and 7 eigenmodes within the waveguide band. The necessary conditions, power conservation ( $|S_{11}|^2 + |S_{21}|^2 = 1$ ) and reciprocity ( $S_{21} = S_{12}$ ), are both satisfied to within 0.001%. Three practical structures, such as CPW-finline transition, CPW gap, and symmetric notch, are chosen to show the influence of metallization thickness on the magnitude and the phase of the scattering parameters. The frequency dependence of the scattering parameters with a fixed separation distance,  $L_0$ , between two cascaded discontinuities is shown in Fig. 3. For a given operation frequency, the dependence of the scattering parameters upon separation distance is illustrated in Figs. 4, 5, 6.

For these three structures, the reflection coefficient  $S_{11}$  is reduced by a thicker metallization when either a CPW mode or a coupled-slot mode is incident. The reduction of the



(a)

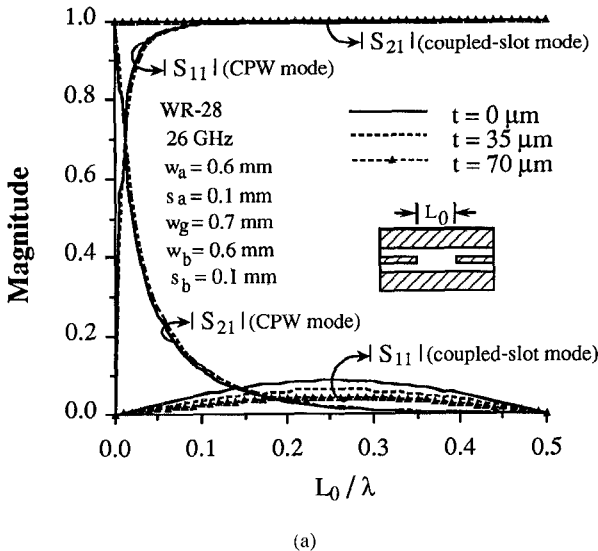


(b)

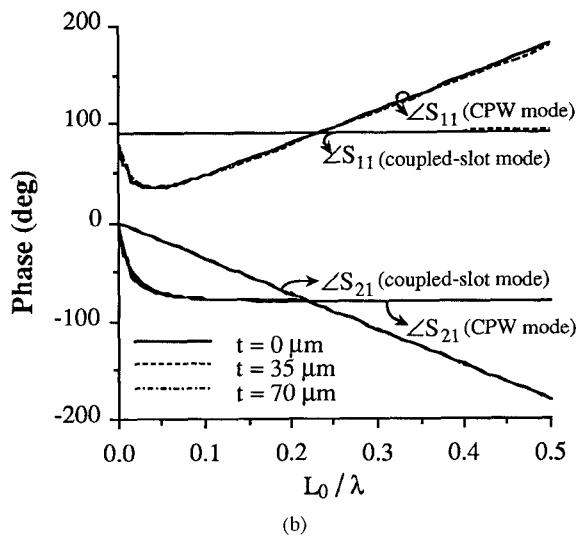
Fig. 4. Scattering parameters of a CPW-finline transition for a coupled-slot mode incident at 26 GHz, (a) magnitude, (b) phase.

reflection coefficient implies that more energy is transmitted through the cascaded discontinuities for a thicker metallization. This phenomenon can be explained by Kuo's parallel-plate waveguide model [3]. A thicker metallization forms a wider parallel-plate waveguide to guide more energy through the slot, therefore; the reflection coefficient is reduced. Another interesting observation is that the metallization thickness has smaller influence on the scattering parameters when the operation frequency is near the end of waveguide band, 26.5 GHz, for a waveguide cutoff frequency at 21.081 GHz. This behavior is similar to the variation of the effective dielectric constant calculated by Kitazawa [1].

From Figs. 4, 5, 6, a periodic variation of the scattering parameters is observed for an incident coupled-slot mode. This periodic variation indicates the existence of a standing wave between the two cascaded discontinuities. For a CPW mode incident in Fig. 5, the transmission coefficient,  $S_{21}$  decreases as  $L_0$  increases, so no standing wave appears in the gap region of a CPW gap. Fig. 5 shows that, for an



(a)



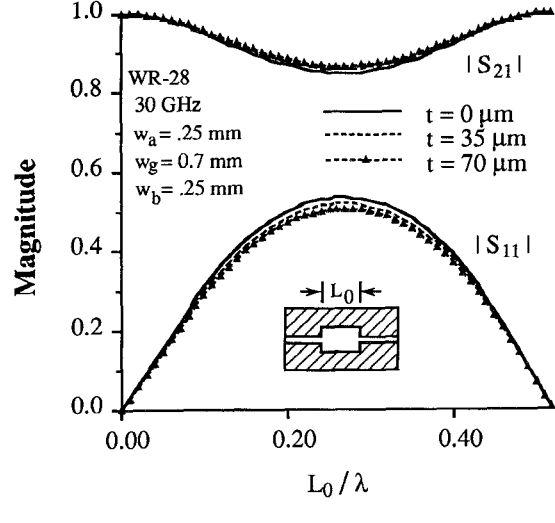
(b)

Fig. 5. Scattering parameters of a CPW gap for a coupled-slot mode and a CPW mode incident at 26 GHz. (a) magnitude, (b) phase.

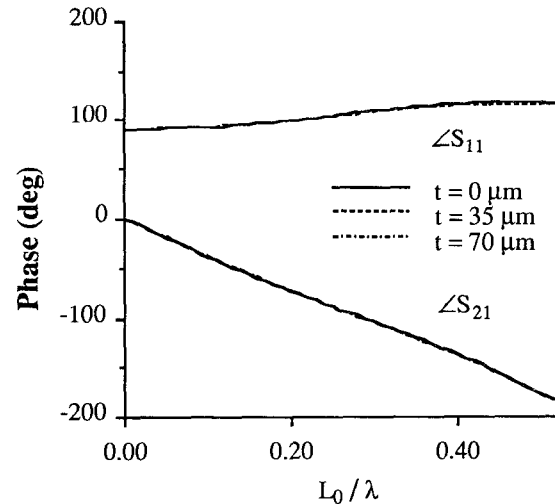
incident coupled-slot mode, the metallization thickness has a more significant influence on the scattering parameters than when a CPW mode is incident on the discontinuities. The standing wave between two cascaded junction discontinuities magnifies the finite metallization thickness effect, especially at a quarter wavelength separation distance,  $L_0 = \lambda/4$ . Although the metallization thickness only has a small influence on the waveguide propagation properties, the resonant behavior in circuits will magnify this small deviation into a large difference on the circuit performance. The metallization thickness effect is significant for both a large resonant circuit in Fig. 6 and a small resonant circuit in Fig. 4. Hence, the metallization thickness effect can not be neglected in MMIC design, especially for a circuit with resonant behavior.

#### IV. CONCLUSION

The analysis of cascaded junction discontinuities of shielded coplanar type transmission line is performed by the mode-matching technique including the effect of finite metallization



(a)



(b)

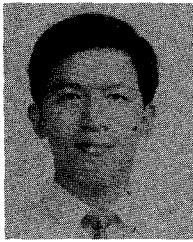
Fig. 6. Scattering parameters of a symmetric notch for a coupled-slot mode incident at 30 GHz. (a) magnitude, (b) phase.

thickness. The transition length dependence and the frequency dependence of the scattering parameters of CPW-finline transition, CPW gap, and symmetric notch, are presented. The accuracy of numerical results is checked by comparisons with published results and several convergence tests. The numerical results indicate that the metallization thickness effect can be magnified by the standing wave between two cascaded junction discontinuities, especially at a quarter wavelength separation distance.

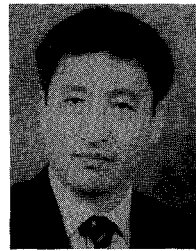
#### REFERENCES

- [1] T. Kitazawa and R. Mittra, "Analysis of finline with finite metallization thickness," *IEEE Trans. Microwave Theory Tech.*, vol. MTT-32, pp. 1484-1487, Nov. 1984.
- [2] R. Vahldieck and W. J. R. Hoefer, "The influence of metallization thickness and mounting grooves on the characteristics of finlines," in *IEEE MTT-S Int. Microwave Symp. Dig.*, 1985, pp. 143-144.
- [3] C. W. Kuo and T. Itoh, "Characterization of shielded coplanar type transmission line junction discontinuities incorporating the finite metallization thickness effect," *IEEE Trans. Microwave Theory Tech.*, vol. 40, pp. 73-80, Jan. 1992.

- [4] C. Shih *et al.*, "Frequency-dependent characteristics of open microstrip lines with finite strip thickness," *IEEE Trans. Microwave Theory Tech.*, vol. 37, pp. 793-795, Apr. 1989.
- [5] L. Zhu and E. Yamashita, "New method for the analysis of dispersion characteristics of various planar transmission lines with finite metallization thickness," *IEEE Microwave Guided Wave Lett.*, vol. 1, pp. 164-166, July 1991.
- [6] W. Heinrich, "The slot line in uniplanar MMIC's: propagation characteristics and loss analysis," in *IEEE MTT-S Int. Microwave Symp. Dig.*, 1990, pp. 167-170.
- [7] L. E. Dikens and D. W. Maki, "An integrated-circuit balanced mixer, image and sum enhanced," *IEEE Trans. Microwave Theory Tech.*, vol. MTT-23, pp. 276-281, Mar. 1975.
- [8] Q. Xu, K. J. Webb and R. Mittra, "Study of modal solution procedures for microstrip step discontinuities," *IEEE Trans. Microwave Theory Tech.*, vol. 37, pp. 381-387, Feb. 1989.



**Tian-Wei Huang** received the B.S. degree in electrical engineering from National Cheng Kung University, and the M.S. degree in electrical engineering from University of California, Los Angeles, in 1987 and 1990, respectively. Since 1991, he has been a Research Assistant with the Department of Electrical Engineering at University of California, Los Angeles.



**Tatsuo Itoh** (S'69-M'69-SM'74-F'82) received the Ph.D. Degree in Electrical Engineering from the University of Illinois, Urbana in 1969.

From September 1966 to April 1976, he was with the Electrical Engineering Department, University of Illinois. From April 1976 to August 1977, he was a Senior Research Engineer in the Radio Physics Laboratory, SRI International, Menlo Park, CA. From August 1977 to June 1978, he was an Associate Professor at the University of Kentucky, Lexington. In July 1978, he joined the faculty at the University of Texas at Austin, where he became a Professor of Electrical Engineering in 1981 and Director of the Electrical Engineering Research Laboratory in 1984. During the summer of 1979, he was a guest researcher at AEG-Telefunken, Ulm, West Germany. In September 1983, he was selected to hold the Hayden Head Centennial Professorship of Engineering at The University of Texas. In September 1984, he was appointed Associate Chairman for Research and Planning of the Electrical and Computer Engineering Department at The University of Texas. In January 1991, he joined the University of California, Los Angeles as Professor of Electrical Engineering and holder of the TRW Endowed Chair in Microwave and Millimeter Wave Electronics and is co-Director of Joint Services Electronics Program.

Dr. Itoh is a member of the Institute of Electronics and Communication Engineers of Japan, Sigma Xi, and Commissions B and D of USNC/URSI. He served as the Editor of *IEEE Transactions on Microwave Theory and Techniques* for 1983-1985. He serves on the Administrative Committee of IEEE Microwave Theory and Techniques Society. He was Vice President of the Microwave Theory and Techniques Society in 1989 and President in 1990. He is the Editor-in-Chief of *IEEE Microwave and Guided Wave Letters*. He also serves on IEEE TAB Periodicals Council and Publications Board as Division IV Representative for 1992-93. He was the Chairman of USNC/URSI Commission D from 1988 to 1990 and is the Vice Chairman of Commission D of the International URSI.